Circularly symmetric soliton states and excitations in an annular Josephson junction

1992 J. Phys.: Condens. Matter 4 4653

(http://iopscience.iop.org/0953-8984/4/19/008)

J. Phys.: Condens. Matter 4 (1992) 4653–4666. Printed in the UK

Circularly symmetric soliton states and excitations in an annular Josephson junction

Qianghua Wang†, Wei Wang†‡§ and Xixian Yao†§

† Physics Department, Nanjing University, Nanjing 210008, People's Republic of China
‡ CCAST (World Laboratory), PO Box 8730, Beijing 100080, People's Republic of China
§ The Centre of Non-linear Dynamical Systems, Nanjing University, Nanjing 210008, People's Republic of China

Received 15 July 1991, in final form 6 January 1992

Abstract. We discuss the circularly symmetric soliton states and the I–V characteristics of an annular Josephson junction with a large width by direct numerical simulation. By assuming a soliton or multiple-soliton solution initially, we find that there exist a stable single-soliton (one-soliton) state, two-soliton state and three-soliton state in our system in the absence of an external applied field. The corresponding zero-field steps are obtained. A state that traps initially more than four solitons in the system turns out to be unstable. There exists a transition between the multiple-soliton states which suggests some physical points for the application of an annular junction. A suggestion of soliton excitation in a physical experiment is also discussed.

1. Introduction

The topic of fluxons in large Josephson junctions has attracted considerable interest. A Josephson junction is a well understood solid system on which experiments can be undertaken with relative ease. There has been a variety of suggestions for applications with such diverse fields as microwave oscillators, amplifiers and data-processing systems [1, 2]. Recently, the Josephson junction has also been researched for the rich non-linear phenomena, such as chaos and phase locking in such a system [3–5]. The relative local pair phase difference across a Josephson junction obeys the modified sine–Gordon equation (SGE). A large junction compared with the Josephson penetration length λ_J can support resonant propagation of a soliton (or fluxon) trapped within the junction. The DC manifestation of these motions is a sequence of equidistantly spaced branches in the I–V characteristic of the junction.

So far attention has been primarily given to one-dimensional (1D) junctions of in-line and overlap types. From our point of view, two-dimensional junctions are no less interesting than 1D junctions in that, under certain conditions and configurations, they can also support soliton motion, and there exists the soliton return effect, e.g. in rotational symmetric junctions, in contrast with the 1D case [6–8]. The main problem for the application of a circular junction with rotational symmetry, from our point of view, is the instability of the soliton at the centre of the junction. After energy radiation from it during its reflection at the centre of the junction, the soliton disappears [8]. A proper

0953-8984/92/194653 + 14 $04.50

way to remove such an obstacle is to excavate the central part of the circular junction. This kind of device (or annular junction) has been studied in the literature in recent years, and also in experiments [9]. However, [9] considered only the problem of tangential rather than radial dynamics of the annular junction which is somewhat equivalent to the 1D overlap junction with spatial periodicity, since the width W of the annular junction there is less than λ_J. If $W \gg \lambda_J$, the self-field effect of the system arises, which introduces the radial dynamics of the junction. Stable circularly symmetric states are special states that may appear and are of great interest. These states may be tunable by both the feeding current and the applied field introduced simply by the current flowing along another wire located at the centre of the junction, without breaking the circular symmetry.

In our previous research [6–8], we have studied the dynamical behaviour of an annular junction in the case of circular symmetry. As was described there, the annular junction is somewhat like an in-line junction with the current introduced at the external boundary. We found that there exists a ring-shaped soliton solution. The dynamical equations and energy equations of the soliton have been obtained in [10] from an energy analysis, which governs the soliton motion. The internal radius ρ_i was set to be very large, and the dissipative parameter α very small; thus the soliton wave is essentially unchanged compared with that in a 1D junction, and the effects of dissipation and the so-called $1/\rho$ term in the SGE are only to modulate the velocity and the position of the soliton. There exist two kinds of soliton motion within the junction.

(i) The first is a resonant soliton motion. A soliton firstly moves inwards and becomes an anti-soliton after the reflection at the internal boundary; then the anti-soliton moves outwards. If the energy is large enough, the anti-soliton will become a soliton after the reflection at the external boundary. The repeated back-and-forth motion within the junction under various feeding currents corresponds to a current step in the I–V characteristic of the junction.

(ii) The second is the returning motion of a soliton. The anti-soliton (or soliton) will return without reaching the external boundary because of not enough energy. That phenomenon is called the soliton return effect [7, 8]. The studies made in [7] were made by direct numerical simulation, and dissipation was not presented there. Considering that the effects of dissipation are unavoidable in a real system, we shall further discuss the soliton return effect (which is considered in particular in the presence of dissipation in [11]) and shall discuss the critical point, the non-zero minimum voltage and current in the current step of the I–V characteristic that relates to the soliton return effect. The soliton return effect makes a main difference between a 1D and an annular junction.

It has been shown by direct numerical simulation as well as experiments that there are multiple-soliton states in both an in-line and an overlap 1D junction [12], although some difference exists between the ranges of the bias current in the zero-field steps (ZFS). From our point of view, there should also exist multiple-soliton states in an annular junction for the similarity between a 1D in-line junction and a circularly symmetric annular junction (which, hereafter, is called annular junction for short). In a numerical simulation, a soliton solution is assumed to be the initial condition. However, in a real system, the soliton could only be excited under certain conditions. There have been experiments on the excitation and behaviour of soliton(s) or fluxon(s) in a 1D long Josephson junction [13, 14], but no experiment on the excitation of a circularly symmetric soliton. Thus it is important to find the way to excite soliton(s) in an annular junction. In addition, the phenomenon of the transition between multiple-soliton states

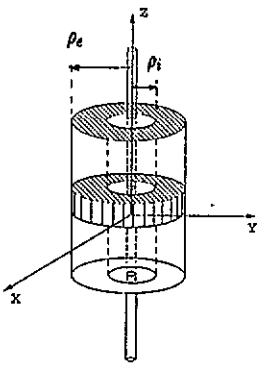

Figure 1. The annular Josephson junction configuration. The annular width W is equal to the difference between the external radius ρ_e and internal radius ρ_i of the junction. The feeding current I' flows along the Z direction, the normal direction of the junction plane. The external magnetic field is produced by a current I'_H that flows along the Z direction in another conducting wire located at the centre of the junction.

deserves to be researched because of its application in the realization of a data-processing system.

The purpose of the present paper is to investigate numerically the single- and multiple-soliton states, to discuss the transition between multiple-soliton states in an annular junction, and to discuss a possible method of soliton excitation. All states are circularly symmetric.

2. Model of simulation

The annular Josephson junction configuration is shown in figure 1. The annular width W is equal to the difference between the external radius ρ_e and internal radius ρ_i of the junction. The feeding current I' flows along the Z direction, the normal direction of the junction plane. The external magnetic field is produced by a current I'_H that flows along the Z direction in another conducting wire located at the centre of the junction. The dimensionless dynamical equation is assumed to be described by the modified SGE [6]

$$\varphi_{\rho\rho} + (1/\rho)\varphi_\rho - \varphi_{tt} - \alpha\varphi_t = \sin\varphi \tag{1}$$

with the boundary conditions

$$\varphi_\rho|_{\rho=\rho_i} = I'_H/2\pi\rho_i \tag{2}$$

$$\varphi_\rho|_{\rho=\rho_e} = (I' + I'_H)/2\pi\rho_e. \tag{3}$$

The normalization of equations (1)–(3) can be found in [6]. In equation (1), φ_ρ and φ_t are the differentials for the phase φ with respect to space ρ and time t respectively, and $\alpha\varphi_t$ represents the dissipation effect which results from the tunnelling of the normal electrons across the barrier. Equations (2) and (3) result from Ampère's law for φ_ρ and I'_H and I', since φ_ρ represents the local magnetic field in our system. The renormalized current I will be used unless confusion might arise: $I = I'/\pi(\rho_e^2 - \rho_i^2)$.

The energy of the junction is [6, 10, 11]

$$E = \int 2\pi\rho \, d\rho \, [\tfrac{1}{2}(\varphi_t^2 + \varphi_\rho^2) + 1 - \cos\varphi] \tag{4}$$

where $\frac{1}{2}(\varphi_t^2 + \varphi_\rho^2)$ is the contribution of the electromagnetic field in the junction, and $1 - \cos\varphi$ is the contribution of the junction free energy due to the existence of supercurrent $\sin\varphi$. The consideration of energy of the junction is useful to discuss the condition of a stable soliton motion, as presented in [10].

We assume that a circularly symmetric soliton solution can be taken as a zeroth-order initial solution of the modified SGE, i.e. equation (1):

$$\varphi = 4\sum_{i=1}^{m}\tan^{-1}\left[\exp\left(\frac{\sigma_i[\rho - R_i(t)]}{(1-u_i^2)^{1/2}}\right)\right. \tag{5}$$

$$\varphi_t = \sum_{i=1}^{m}\left[-\frac{2\sigma_i u_i}{(1-u_i^2)^{1/2}}\operatorname{sech}\left(\frac{\sigma_i[\rho - R_i(t)]}{(1-u_i^2)^{1/2}}\right)\right] \tag{6}$$

where $\sigma_i = \pm 1$ are the polarities of the soliton and anti-soliton respectively, and m is the number of solitons (or anti-solitons). Hereafter, we shall not identify the soliton or anti-soliton unless confusion might arise. The function $R_i(t)$ describes the radius of the fluxon, i.e. the maximum of φ_t, and will be simply denoted hereafter as R_i. In fact, the exact solution of equation (1) differs (but not essentially) from that described by equations (5) and (6) and thus should be called the exact quasi-soliton solution. For convenience, we would rather call them the soliton or multiple-soliton solution instead.

Since dissipation exists in our system, the initial values of σ_i and u_i should be chosen appropriately with respect to I to ensure that the net energy input is positive to balance the dissipation.

We use the implicit finite-difference method with respect to space ρ, and the fourth-order Runge–Kutta integration with respect to time t together with the initial conditions, equations (5) and (6), to evaluate the evolution of the discretized φ and φ_t, etc. The algorithm is described in more detail in the appendix. The precision and stability of computation are carefully checked in case any artificial results might arise. In our double-precision computation, the step $\delta\rho$ in space and the step δt in time are 0.1 and 0.05, respectively, which already provide satisfactory precision and computation stability. The average voltage of the junction is given by

$$V = \langle\varphi_t\rangle_{t\rho} \tag{7}$$

which is the spatial–temporal average of φ_t.

3. Results and discussion

Throughout the following discussion, we deal with the annular junction with $\rho_i = 20$ and $\rho_e = 30$ in the absence of an external field ($I_H = 0$). The dissipation constant is $\alpha = 0.01$ unless it is specially defined. The reason for the choice of α is as follows: explicitly, $\alpha \approx \lambda_J/c'R_NSC$ where c' is the speed of light in the oxided medium, R_N is the normal resistance of the junction, S is the area of the junction and C is the capacity per unit area. Typical values of the parameters are [15] $\lambda_J \approx 10^{-2}$ cm, $c' \approx 10^9$ cm s^{-1}, $R_NS \approx 10^{-4}\,\Omega$ cm^2 and $C \approx 10^{-5}$ F cm^{-2}; hence a typical value of α is 10^{-2}. In our simulation, a stable state obtained under a certain bias current I is used as the initial condition under another adiabatically varied bias current I with respect to the former bias current. Thus the I–V characteristics of the junction can be easily obtained.

3.1. Single-soliton state

Taking $m = 1$, $\sigma_1 = +1$, $u_1 = -0.94$ and $R_1 = 28$ in the initial conditions described by equations (5) and (6), we find that a single-soliton state is stable under the bias current

in the range $0.013 < I < 0.078$. We discuss the stable soliton state under a bias current of $I = 0.022$ (or $I' = 35$) as an example.

Figure 2(*a*) shows the soliton solution $\varphi_\rho \sim \rho$ at successive moments. The polarity σ changes after the reflection of the soliton (or anti-soliton) at the boundaries. However, the sign of $-u\sigma$ does not change; thus from equation (6) we see that the sign of φ_t would not change, $I\varphi_t$ would remain positive and the junction could get a positive energy input from the boundary to balance the dissipation in the junction. To see this, we present figure 2(*b*) which shows the relation $\varphi_t \sim \rho$ at successive moments corresponding to figure 2(*a*). We see that φ_t remains positive during the back-and-forth motion of the soliton, except for some small amplitude waves or fluctuations which, in our view, result from the $1/\rho$ term in equation (1).

The reflection of a soliton at each boundary can be assumed to be a collision process between a soliton within the junction and a virtual anti-soliton outside, and vice versa [16]. Thus φ_ρ becomes very small but φ_t becomes relatively large when the soliton is reflected. This can be seen from figures 2(*a*) and 2(*b*). Therefore it is advisable for us to take the position of the maximum of φ_t as the central position R of the soliton to discuss the dynamical behaviour of a soliton. We have given by means of an energy analysis in [10, 11] a full presentation of the equations that govern the dynamical behaviour of a soliton. Here we present only our results of direct numerical simulation. Figure 2(*c*) shows the evolution of the central position R of the soliton versus time t. Although dissipation exists in the junction, the velocity of the soliton is hardly changed during its motion. However, if the dissipation is slightly larger, for instance, $\alpha = 0.04$ (and $I = 0.06$), the situation is different; the relation $R \sim t$ is shown in figure 2(*d*) from which we can see that in this situation the velocity of the soliton is hardly changed during its motion from ρ_e to ρ_i but is decreased markedly during its motion from ρ_i to ρ_e. This behaviour cannot be explained only in terms of dissipation, as in the case of a 1D in-line junction. In [10, 11], we explain the behaviour as the co-action of the dissipation and the so-called 'effective attracting force' acting upon the soliton. The attracting force results from the $1/\rho$ term in equation (1), and it always tends to make the soliton move inwards. In fact, the dynamical equation of the soliton motion is [10]

$$\mathrm{d}u/\mathrm{d}t \sim -(1/R)(1-u^2) - \alpha u(1-u^2) \tag{8}$$

with

$$\mathrm{d}R/\mathrm{d}t = u \tag{9}$$

where $\mathrm{d}u/\mathrm{d}t$ is the acceleration of the soliton, and $|u| < 1$ (1 is the speed of light in the barrier). We can see from equation (8) that it depends on the competition of the attraction and the dissipation whether or not the velocity of the soliton is decreased during the motion inwards (with $u < 0$). Also, from equation (8), it is obvious that the velocity is decreased in any case during the outward motion (with $u > 0$). Because of the action of the attracting force, the soliton would return before it reaches the external boundary if its initial velocity were not large enough. This phenomenon is called the soliton return effect [8, 11], which occurs when the external radius is too large or the bias current is not large enough to input enough energy into the junction; so the velocity of the soliton decreases with the decrease in energy due to dissipation. The soliton return effect in the presence and absence of dissipation will be discussed in detail elsewhere [11]. In figures 2(*c*) and 2(*d*) there are some irregular regions which result from our definition of R and the existence of fluctuations (or small-amplitude waves) in the junction. The irregularity becomes even more prominent when the soliton is in the

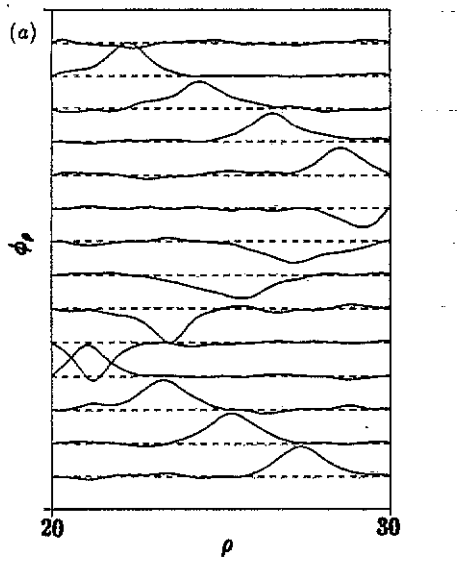

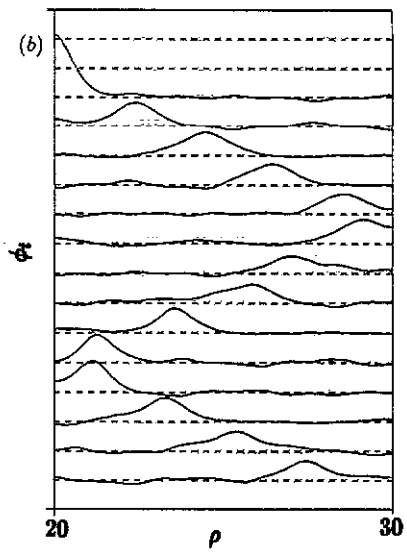

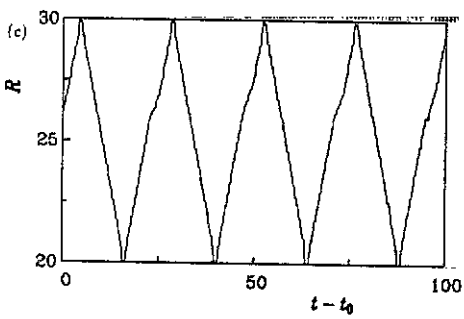

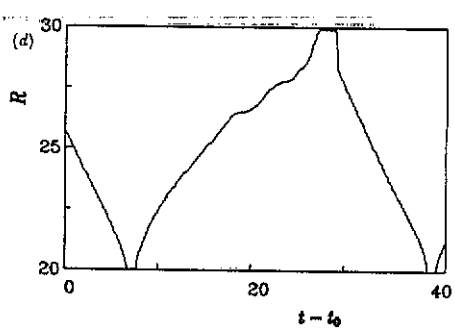

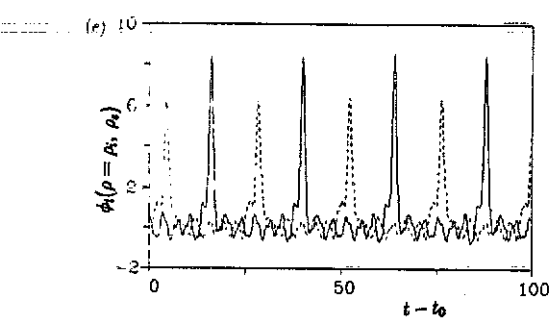

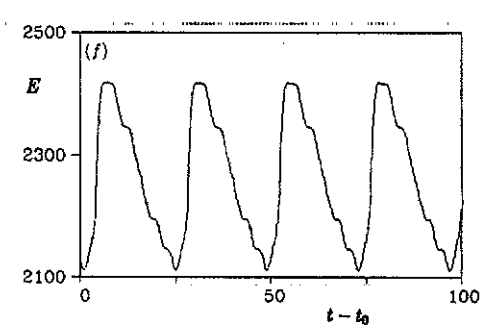

Figure 2. Continued on the following page.

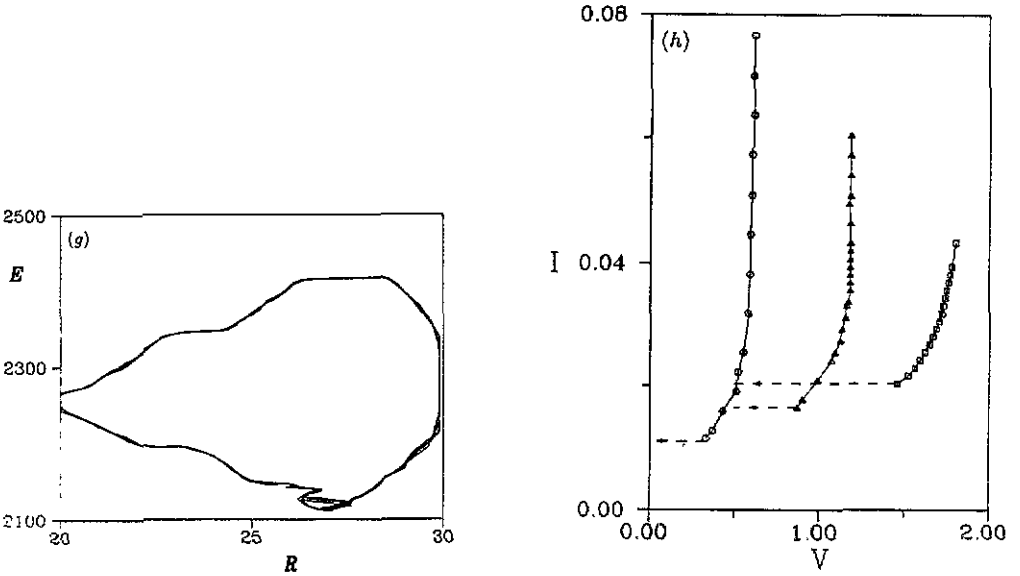

Figure 2. (*a*) The soliton solution $\varphi_\rho \sim \rho$ under a feeding current of $I = 0.022$ at successive moments with a time interval of $\Delta t = 2.5$ (normalized). The axis of $\varphi_\rho = 0$ is shifted upwards with increase in time (---) with a spacing of $\Delta\varphi_\rho = 4$. The scale of each curve is the same. The junction parameters are $\rho_i = 20$, $\rho_e = 30$ and $\alpha = 0.01$. (*b*) The relation $\varphi_t \sim \rho$ corresponding to (*a*); the spacing between the broken lines is $\Delta\varphi_t = 4$. (*c*) The t-dependence of the central position R of the soliton. The parameters of the junction are the same as in (*a*), and t_0 is an initial value of t. (*d*) The same as (*c*) except that here the dissipation is $\alpha = 0.04$, and t_0 is another initial value of t here. (*e*) The t-dependence of the voltage signal φ_t at the boundaries with $\rho = \rho_i$ (——) and $\rho = \rho_e$ (---) respectively. The junction parameters and t_0 are the same as those in (*c*). (*f*) The t-dependence of junction energy E. The junction parameters and t_0 are the same as those in (*c*). (*g*) The relation between the junction energy E and the central position R of the soliton. The junction parameters are the same as those in (*a*). (*h*) The ZFSs of the junction: ○, 1-ZFS; △, 2-ZFS; □, 3-ZFS. The parameters are the same as those in (*a*): $\alpha = 0.01$, $\rho_i = 20$ and $\rho_e = 30$. The broken line and the arrows are a guide to the transition of the soliton states at the upper and lower ends of each branch.

vicinity of the boundaries ($R \sim \rho_i$ or $R \sim \rho_e$), owing to the action of the boundaries upon the soliton.

Figure 2(*e*) shows the evolution of $\varphi_t(\rho = \rho_i)$ (full curve) and $\varphi_t(\rho = \rho_e)$ (broken curve) versus time t. The periodicity is obvious. From figures 2(c) and 2(*e*), we can see that a voltage pulse is created at a boundary where the soliton is reflected; therefore, the junction radiates energy periodically. The periodicity, high frequency and possibly large power of radiation make it reasonable for the application of an annular junction as a microwave oscillator.

The variation in the energy E of the junction versus time t and central position R of the soliton is shown in figures 2(*f*) and 2(*g*). There is an irregular region in figure 2(*g*) which results from our definition of R and the existence of fluctuations in the junction, as mentioned above. As no external applied field ($I'_H = 0$) exists, the soliton does not get an energy input at the internal boundary but does in the vicinity of the external boundary, qualitatively in accordance with the analytical discussion in [10] which indicated that, in the absence of applied field, $\Delta E_i = 0$ and $\Delta E_e = 4\pi I'$ where ΔE_i and ΔE_e are the energy changes due to the reflection of the soliton at the internal and external

boundaries, respectively. The energy decreases when the soliton moves within the junction because of dissipation. The consideration of the balance between the net energy input and dissipation can be employed to determine the condition of a stable soliton motion. This is the main idea used in [10, 11].

The variation in φ at any position ρ, from our numerical results, is 4π in the time interval of one period of back-and-forth motion of the soliton. This confirms that the soliton here has also the characteristic of a 2π kink. Therefore, the average voltage $V = \langle\varphi_t\rangle_{t\rho}$ equals, for a single-soliton state, $4\pi/T$ where T is the period of the soliton motion.

So far, we have discussed the single-soliton state under a bias current of $I = 0.022$. Figure 2(h) shows the ZFS with respect to any stable soliton and multiple-soliton states, and the 1-ZFS is shown as open circles. The range of bias current of the 1-ZFS is $0.011 < I < 0.078$. If $I < 0.011$ the soliton state is unstable; after several turns of return process, the soliton disappears, and the average voltage V is zero. This corresponds to the switch from the finite-voltage state (soliton mode) to the zero-voltage background, i.e. to the axis $V = 0$ in figure 2(h). This transition, which has been discussed analytically in [11], is discontinuous and gives a critical situation with non-zero minimum current and voltage at the lower end of the 1-ZFS, and relates to the so-called soliton return effect. This phenomenon is remarkably different from the case of the 1D junction, for which V on the 1-ZFS varies discontinuously to zero theoretically only if the dissipation is taken into account during the collision process of soliton and virtual anti-soliton (or vice versa) at the boundary [17] (for the corresponding experiments, see [18]). In other words, there are two effects, namely dissipation and the soliton return effect, which contribute to the non-zero voltage phenomenon at the lower end of the ZFS in our system. On the other hand, if $I > 0.078$, the state switches to a rotational state in which the phase φ increases very rapidly with a nearly constant 'angular velocity' ω, i.e. $\varphi \sim \varphi_0 + \omega t$ where φ_0 is an initial value of φ. This transition corresponds to the switch from soliton state (soliton mode) to ohmic background. The rotational state of an annular junction has been discussed elsewhere [6].

3.2. Two-soliton state

As an initial condition, we take $m = 2$, $\sigma_1 = \sigma_2 = +1$, $u_1 = u_2 = -0.94$, $R_1 = 24$ and $R_2 = 28$. Following the same procedure as in section 3.1, we find that in the range $0.016 < I < 0.060$, the two-soliton state is stable. The corresponding 2-ZFS is shown in figure 2(h) (open triangles). Figure 3(a) shows the two-soliton solution $\varphi_\rho \sim \rho$ at successive moments under a bias current of $I = 0.033$, and figure 3(b) shows the relation $\varphi_t \sim \rho$ correspondingly. We can see from figure 3(a) that the solitons move along the same direction when their polarities are the same, and vice versa. When the two solitons collide, the local magnetic field φ_ρ is reduced, but the local voltage φ_t is increased. The above-mentioned behaviour of the polarities and velocities of the solitons considered can be well understood from equation (6). Figure 3(c) shows the t-dependence of $\varphi_t(\rho = \rho_e)$. The pulses correspond to the reflection of the solitons at the boundary. We can see from figures 2(a) and 2(b) that the solitons are separated a nearly constant distance of 4–5 λ_J when they move along the same direction, as if no interaction exists. To clarify the interaction between the solitons, firstly we initially locate the solitons closely (e.g., a distance of 1–2 apart) or simply take the superposition of two solitons; with the same polarity and direction of velocity, we find that finally the solitons are a distance of 4–5 λ_J apart when they are in motion. Secondly, we initially separate the solitons a long distance of 6–7 λ_J (compared with the width of the junction, $W = 10$); with the same polarity and

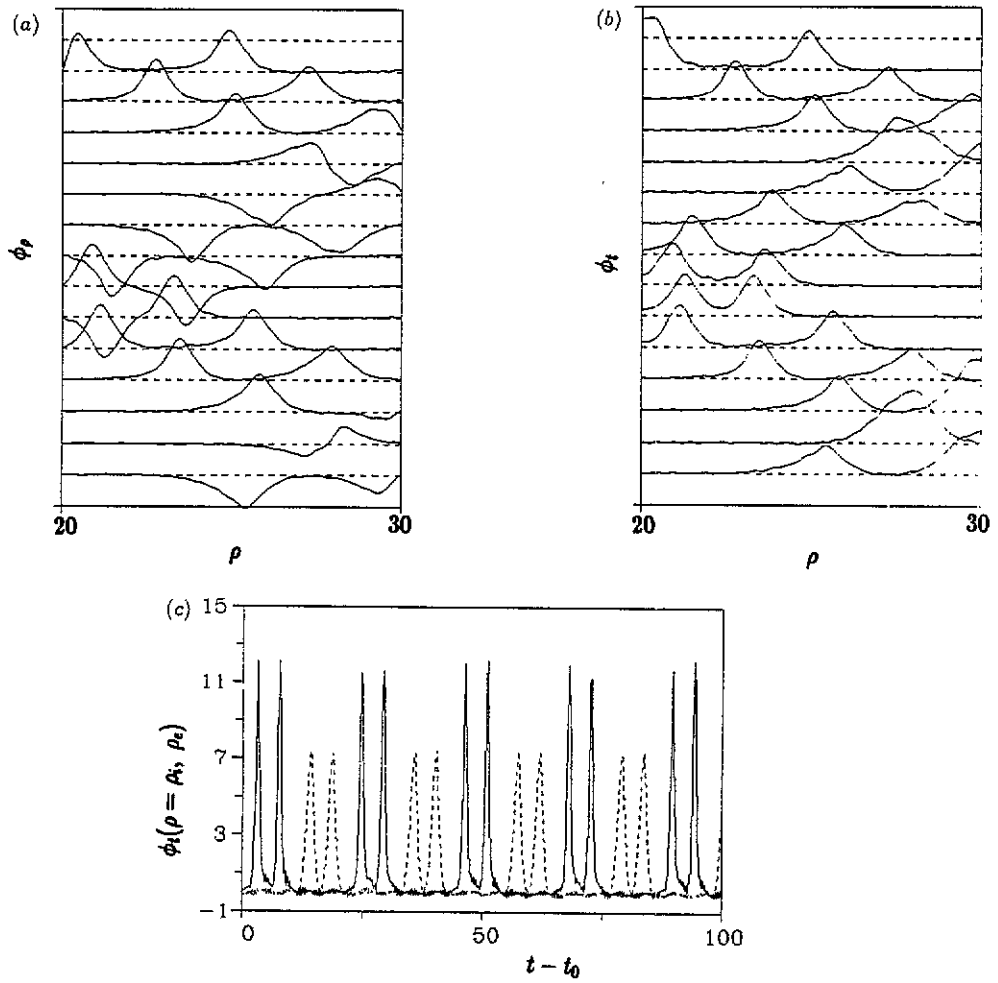

Figure 3. (*a*) The same as figure 2(*a*) except that it is a two-soliton solution, and the bias current is $I = 0.033$. (*b*) The relation $\varphi_t \sim \rho$ corresponding to (*a*). (*c*) The t-dependence of the voltage signal φ_t at the boundaries with $\rho = \rho_i$ (——) and $\rho = \rho_e$ (– – –) in a two-soliton state under the bias current of $I = 0.033$, with t_0 an initial value of t here.

direction of velocity, we find that finally the solitons are again a distance of 4–5 λ_J apart. Thus we can conclude that interaction exists between the solitons, and a distance exists between the solitons when the interaction is zero.

The radiation of the junction in a two-soliton state is similar to that in the one-soliton state except that there are two voltage pulses at each boundary during a period because of the reflection of each soliton, as can be seen from figure 3(*c*). From figure 3(*c*) we can also conclude that the two solitons are not in the so-called standing-wave mode, but in a propagating mode. Otherwise, there would be synchronized variation of φ_t at each boundary [19]. The reason is that the boundary condition is neither symmetric nor asymmetric; it is impossible to excite a standing-wave mode. The average voltage of the junction in a two-soliton state equals $8\pi/T$ where T is the period of the state, since φ at any position changes by 8π during a period.

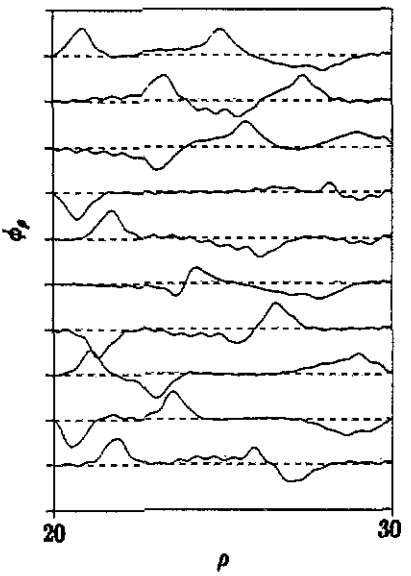

Figure 4. The same as figure 2(*a*) except that it is a three-soliton solution; the bias current is $I = 0.03$, and the spacing between the broken lines (the axis with $\varphi_\rho = 0$) is 10.

From the stable two-soliton state under the minimum bias current $I = 0.016$, with a decrease in I, two cases may occur.

(i) If the decrease is slightly large, e.g. $\Delta I' = 4$, then the state switches to a zero-voltage state even if the bias current is still in the range of 1-ZFS.

(ii) If the decrease is small enough, e.g. $\Delta I' = 1$, then the former state switches to a one-soliton state, as indicated by the broken curve in figure 2(*h*).

On the other hand, if we increase the bias current from the stable two-soliton state under the maximum bias current $I = 0.06$, the former state switches to a rotational state. However, this rotational state is more complicated than that discussed in [6], since it is not periodic. Chaos or intermittency may exist in such a state. We shall discuss this elsewhere.

3.3. Three-soliton state

Taking $m = 3$, $\sigma_1 = \sigma_2 = \sigma_3 = +1$, $u_1 = u_2 = u_3 = -0.9$, $R_1 = 28$, $R_2 = 26$ and $R_3 = 22$ in equations (5) and (6) as an initial condition, we find that the three-soliton state is stable in the bias current range $0.02 < I < 0.043$. The corresponding 3-ZFS is shown in figure 2(*h*) as open squares. The average voltage V equals $12\pi/T$ where T is the period of the state under a certain bias current. However, in such a state, $\sigma_1\sigma_2\sigma_3 = -1$, i.e. there is always a soliton with a polarity different from those of the others. This can be seen in figure 4 which shows the solution $\varphi_\rho \sim \rho$ at successive moments under a bias current of $I = 0.03$. We would like to emphasize that the three-soliton state here is not in the symmetric standing-wave mode. The reason is similar to the case of the two-soliton state.

With the slow decrease in I at the lower end of the 3-ZFS, the three-soliton state switches to a one-soliton state, but never to a two-soliton state in our case. A pair of solitons disappears. On the other hand, with increase in I at the upper end of the 3-ZFS,

the three-soliton state switches to a complicated rotational state, similar to the transition of the two-soliton state.

We can see from figure 4 that there are many small waves, or fluctuations in the solution, which in our view, result from the $1/\rho$ term in equation (1) and the successive reflection of each soliton at the boundaries. A continuous mode is excited when the reflection or soliton collision occurs even in a 1D case [16]. The effect of soliton reflection becomes more and more important with increasing number of solitons. Thus, a state that traps too many solitons would be unstable. This is discussed in the following section.

3.4. The unstable multiple-soliton states, rotational states and soliton excitation

Taking $m = 4$, $\sigma_1 = \sigma_2 = +1$, $u_1 = u_2 = -0.94$, $R_1 = 26$, $R_2 = 22$, $\sigma_3 = \sigma_4 = -1$, $u_2 = u_4 = 0.9$, $R_2 = 24$ and $R_4 = 28$ in equations (5) and (6) as an initial condition, we find that the final state is not a four-soliton state. Varying the parameters in equations (5) and (6) gives the same results. The final state may be a two-soliton state or a non-periodic rotational state, depending on the bias current. We have taken the superposition of a stable three-soliton solution and a stable one-soliton solution as another kind of initial condition; unfortunately no stable four-soliton state has been found. However, the final state may be a stable three-soliton state again in a certain range of bias currents. Therefore, the transition of the assumed four-soliton state depends on the initial condition.

Furthermore, we have taken other initial conditions described by equations (5) and (6) with $10 > m > 4$; as a result, we have not found any corresponding stable multiple-soliton state. The final state is non-periodic because of the random transition between two or more multiple-soliton states. Recently, a study on the chaos in a 1D long Josephson junction without an external RF driving force has been made [5]. It is not impossible for chaos to occur in our system since the boundary conditions, equations (2) and (3), are similar to that of a 1D junction with a DC external field. The chaotic behaviour of the junction can be seen from figure 5, the I–V characteristic in such a state. Figure 5 also shows the hysteresis for increasing current from the upper end of 1-ZFS and decreasing from the periodic rotational state.

Finally, from a rotational state, we get a stable two-soliton state by decreasing the bias current adiabatically to $I = 0.032$ and, by decreasing the bias current further, we get a stable one-soliton state, as indicated in figure 2(h) and figure 5. In [6], we have shown that the rotational states starting from different initial conditions are finally identical. One of the realistic initial conditions is the flat-value condition with $\varphi = 0$ and $\varphi_t = 0$ at any position. Thus the transition from a rotational state to a soliton state suggests that soliton(s) can be excited practically.

4. Summary

We have discussed the stable circularly symmetric multiple-soliton states and the ZFS of the annular junction. The rotational state and the hysteresis in the I–V curve are also mentioned. We find the following.

(i) There exist multiple stable states in the annular junction, namely a zero-voltage state, one-, two- and three-soliton states in the bias region of the 3-ZFS, and the bias range of the ZFS decreases with increase in the number of solitons.

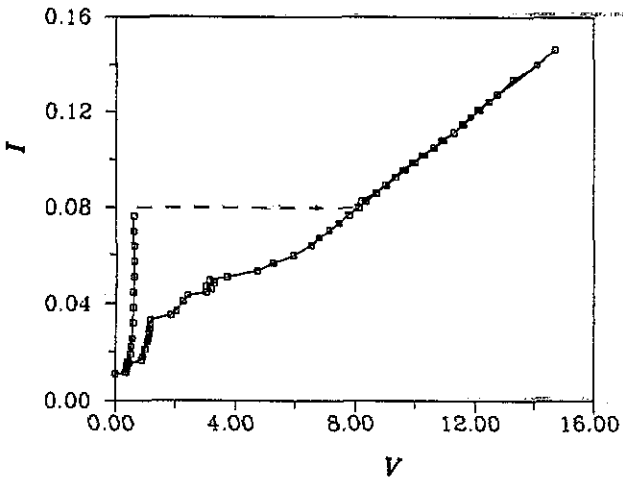

Figure 5. The hysteresis behaviour of the I–V characteristics of the junction for increasing current from 1-ZFS and decreasing current to the zero-voltage state. The lines and arrows are a guide to the eye.

(ii) In the 1-ZFS of an annular junction, the minimum bias current and voltage do not equal zero, and the transition from a single-soliton state to zero-voltage state at the lower end of the 1-ZES is discontinuous. This phenomenon results from special dynamical behaviour, namely the soliton return effect in the annular junction and the effect of soliton reflection at the boundaries discussed in [17, 18]. However, only the latter contributes theoretically to this kind of phenomenon in the 1D case [17, 18].

(iii) There exists a transition between the multiple-soliton states, and a soliton could be excited from a rotational state by decreasing the bias current, i.e. along the hysteresis curve in figure 5.

In addition, it is under our further investigation whether or not the solitons discussed in the present paper remain stable under structural irregularities and tangential electromagnetic perturbation from the outside world. This question is crucial for the experimental observation of such solitons.

Acknowledgment

We would like to acknowledge the support of the Chinese Natural Science Foundation for this work.

Appendix

We describe briefly here the algorithm used in our numerical simulation. The former junction with circular symmetry is divided into N subannular junctions circling the same origin, each with a width $\delta\rho$ and a radius $\rho(j) = \rho_i + (j-1)\,\delta\rho$ where ρ_i is the

internal radius of the former junction, and $j = 1, N$. Therefore, in the interior of the former junction, equation (1) is discretized as

$$(\mathrm{d}/\mathrm{d}t)\varphi_t(j) = [\varphi(j+1) + \varphi(j-1) - 2\varphi(j)]/(\delta\rho)^2 + [\varphi(j+1) - \varphi(j-1)]/[2\rho(j)\,\delta\rho] - \sin[\varphi(j)] - \alpha\varphi_t(j) \tag{A1}$$

where $2 \leqslant j \leqslant N-1$. At the boundaries of the former junction, upon referring to equations (2) and (3), we get

$$(\mathrm{d}/\mathrm{d}t)\varphi_t(1) = [2\varphi(2) - 2\varphi(1) - I'_H\,\delta\rho/\pi\rho_i]/\delta\rho^2 + I'_H/2\pi\rho_i^2 - \sin[\varphi(1)] - \alpha\varphi_t(1) \tag{A2}$$

$$(\mathrm{d}/\mathrm{d}t)\varphi_t(N) = [2\varphi(N-1) - 2\varphi(N) + \delta\rho\,(I'_H + I')/\pi\rho_c]/(\delta\rho)^2 + (I'_H + I')/2\pi\rho_c^2 - \sin[\varphi(N)] - \alpha\varphi_t(N) \tag{A3}$$

where ρ_c is the external radius of the former junction. On the other hand, we have the identity

$$(\mathrm{d}/\mathrm{d}t)\varphi(j) = \varphi_t(j). \tag{A4}$$

For clarity, equations (A1)–(A4) are summarized as

$$(\mathrm{d}/\mathrm{d}t)\boldsymbol{Y} = \mathbf{A}\boldsymbol{Y} + \boldsymbol{F} \tag{A5}$$

where $\boldsymbol{Y} = (\varphi(1), \ldots, \varphi(N); \varphi_t(1), \ldots, \varphi_t(N))^{\mathrm{T}}$, $\mathbf{A}$ is a $2N \times 2N$ matrix, and $\boldsymbol{F}$ is a $2N$-dimensional source-like vector introduced by the feeding current I' and current I'_H, independent of $\varphi(j)$ and $\varphi_t(j)$. Both the vector $\boldsymbol{F}$ and the matrix $\mathbf{A}$ can be fully evaluated from equations (A1)–(A4). Upon using the initial conditions described by equations (5) and (6), we then solve equation (A5) by the fourth-order Runge–Kutta integration method and get the vector flow $\boldsymbol{Y}$ at the subsequent moment. Double precision is used in the computation. Good precision and computation stability are always achieved, as long as $(\delta\rho)^2 \sim \delta t$ and $\delta\rho < 0.1$. (The reader is referred to the literature for a rigorous discussion of the algorithm.)

References

[1] Barone A and Paterno G 1982 *Physics and Applications of the Josephson Effect* (New York: Wiley)
[2] Christiansen P L, Lomdahl P S and Zabusky N J 1981 *Appl. Phys. Lett.* **39** 170
[3] Olsen O H and Samuelsen M R 1985 *Appl. Phys. Lett.* **47** 1007
[4] Mygind J, Olsen O H, Pedersen N F and Samuelsen M R *SQUID-85 Proc. 3rd Int. Conf. on Superconductor Quantum Devices* (Berlin: Walter de Gruyter) 507 pp
[5] Octavio M 1990 *Physica* A **163** 248
[6] Wang Wei, Thomson A L and Yao Xixian 1991 *Phys. Rev.* B **43** 2756
[7] Wang Wei and Yao Xixian 1989 *J. Phys A: Math. Gen.* **22** 2447
[8] Christiansen P L and Olsen O H 1978 *Phys. Lett.* **68A** 185
[9] Davidson A, Dueholm B and Pedersen N F 1986 *J. Appl. Phys.* **60** 1447
[10] Wang Qianghua, Wang Wei and Yao Xixian 1992 *Phys. Rev.* B at press
[11] Wang Qianghua, Wang Wei and Yao Xixian 1991 *J. Appl. Phys.* at press
[12] Pedersen N F and Welner D 1984 *Phys. Rev.* B **29** 2551
[13] Matsuda A 1986 *Phys. Rev.* B **34** 3127
[14] Newman H S and Davis K L 1982 *J. Appl. Phys.* **53** 7026
[15] Likharev K K 1979 *Rev. Mod. Phys.* **51** 101
[16] Maclaughlin D W and Scott A C 1978 *Phys. Rev.* A **18** 1652

[17] Olsen O H, Pedersen N F, Samuelsen M R, Svensmark H and Welner D 1986 *Phys. Rev.* B **33** 168
[18] Pedersen N F and Welner D 1984 *Phys. Rev.* B **29** 2803
[19] Chang Jhy-Jiun 1985 *Phys. Rev.* **31** 1658